A fundamental evaluation of the electrical properties and function of cardiac transverse tubules

Vermij S.H.[a], Abriel H.[a], Kucera J.P.[b]

Affiliations

a. Institute of Biochemistry and Molecular Medicine, University of Bern, Bühlstrasse 28, 3012 Bern, Switzerland.
sarah.vermij@ibmm.unibe.ch, hugues.abriel@ibmm.unibe.ch

b. Department of Physiology, University of Bern, Bühlplatz 5, 3012 Bern, Switzerland.
kucera@pyl.unibe.ch

Corresponding author

Sarah Vermij

Institute of Biochemistry and Molecular Medicine

University of Bern, Bühlstrasse 28, 3012 Bern, Switzerland

E-mail: sarah.vermij@ibmm.unibe.ch

Telephone: +41 31 631 53 52

CONTENTS

ABSTRACT

This work discusses active and passive electrical properties of transverse (T-)tubules in ventricular cardiomyocytes to understand the physiological roles of T-tubules. T-tubules are invaginations of the lateral membrane that provide a large surface for calcium-handling proteins to facilitate sarcomere shortening. Higher heart rates correlate with higher T-tubular densities in mammalian ventricular cardiomyocytes. We assess ion dynamics in T-tubules and the effects of sodium current in T-tubules on the extracellular potential, which leads to a partial reduction of the sodium current in deep segments of a T-tubule. We moreover reflect on the impact of T-tubules on macroscopic conduction velocity, integrating fundamental principles of action potential propagation and conduction. We also theoretically assess how the conduction velocity is affected by different T-tubular sodium current densities. Lastly, we critically assess literature on ion channel expression to determine whether action potentials can be initiated in T-tubules.

KEYWORDS

Myocytes, cardiac; transverse tubules; cardiac conduction; action potential; voltage-gated sodium channels

1. Introduction

Transverse tubules are deep membrane invaginations of the lateral sarcolemma found in all striated muscle cells. In cardiomyocytes from mammalian cardiac ventricles, T-tubules form a particularly complex network throughout the cell [3, 4] (see **Fig. 1**), and are rich in ion channels and many regulatory proteins (reviewed in [5-7]). In atrial cells, the T-tubular network is dense, half-dense, or absent [8]. From the classic dictum "form follows function", it is easy to formulate hypotheses about the function of T-tubules without becoming teleologic. Given that the T-tubular network protrudes deep into the cell, the increase in sarcolemmal surface functions as a platform for signaling and calcium handling [5]. Through T-tubules, signals from extra- to intracellular domains – both electrical and biochemical – can be conducted relatively fast. Indeed, T-tubules are the stage for many different processes (reviewed in [6]).

This work is dedicated to the question what the functional roles of T-tubules are. We discuss the depolarization delay of T-tubular membrane, and the effects of sodium current on membrane potential and electrical potentials in T-tubules. We also discuss principles of physiology in the context of T-tubules, and experimental data in the context of these physiological principles. Since the remodeling of T-tubules is observed in many cardiac diseases [9, 10], it is crucial to understand the roles of T-tubules in healthy cells before we can address the consequences of T-tubular remodeling.

We will only concisely discuss T-tubular structure (**Section 2.2**), signaling (**Section 2.3**), and remodeling in disease (**Section 3.6**), since excellent reviews have already been published on these topics [5-7, 9-11]. Rather, our work will focus on the electrical properties of T-tubules. Firstly, we will discuss the passive properties of T-tubules (**Section 3.1**), that is, the process by which initial depolarization of the cell membrane propagates into

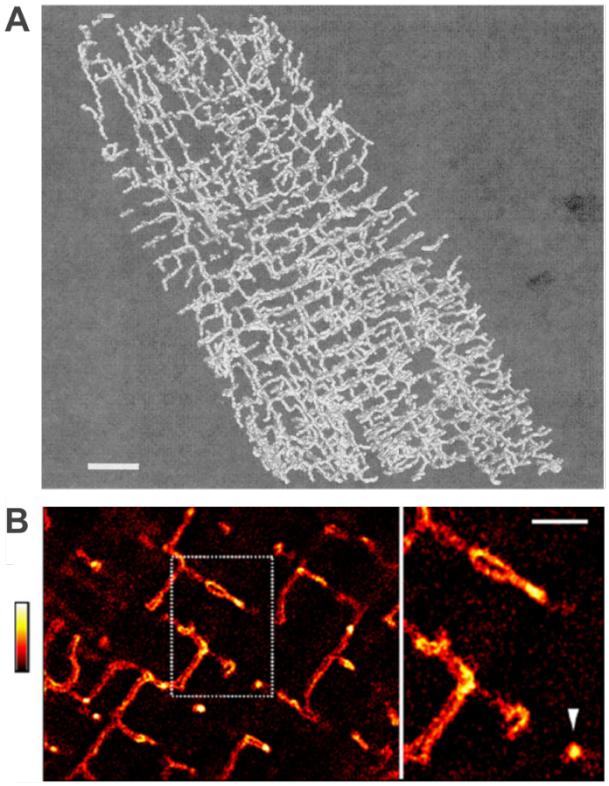

Figure 1. T-tubular structure. (**A**) Two-photon image of T-tubular network in rat ventricular cardiomyocyte. Scale bar: 5 μm. Reprinted from Soeller & Cannell 1999 [1] with authorization of the publisher. (**B**) Transverse and axial elements of the T-tubular network in murine ventricular cardiomyocyte stained with the membrane dye di-8-ANEPPS imaged by stimulated emission depletion (STED) microscopy. Dotted rectangle indicates location of magnified region on the right. White arrowhead indicates a cross-section of a T-tubule. Scale bar: 1 μm; fluorescence intensity given by look-up table on the left. Reprinted from Wagner *et al.* 2012 [2] with authorization of the publisher.

T-tubules without considering voltage-gated ion channels. This includes the discussion of relevant aspects of cable theory [12-16]. Special attention will go out to the capacitive current, which charges the membrane during cell excitation, whereby a larger membrane surface requires more time to charge. To this end, we discuss the delay of T-tubular membrane depolarization. We then assess extracellular potential along the T-tubules and its effect on sodium current amplitude (**Section 3.2**).

Section 3.3 is dedicated to conduction, since conduction velocity is an important parameter in arrhythmogenesis [17] and is affected by the presence of T-tubular membrane and ion channels. Over the course of the upstroke of an action potential, we describe the capacitive current, transmembrane current, and membrane potential changes for a cell. We will then assess theoretically how conduction velocity may differ between tissues with three different densities of T-tubular voltage-gated sodium channels: (1) no or few channels in T-tubules; (2) same channel density in T-tubules as in surface membrane; and (3) higher channel density in T-tubules than in surface sarcolemma.

In **Section 3.4**, we critically review published data on the expression of voltage-gated ion channels and ion pumps, because the data quality is at times unsatisfactory, yet often cited without critical connotations. This will elucidate whether T-tubules contain the necessary collection of ion handling proteins to generate an action potential. Although **Section 3.1** and **3.2** will illustrate that theoretically passive conduction suffices to depolarize the T-tubular membrane quickly enough, action potentials may still be evoked.

Ion dynamics in the T-tubular lumen will be concisely discussed in **Section 3.5**. The small and tortuous T-tubular lumen restricts diffusion and affects driving force of voltage-gated ion channels [18, 19]. Lastly, we will discuss T-tubule heterogeneity in atrial cardiomyocytes in **Section 4**. Atrial cells contract as often as ventricular cells, yet have less T-tubules than ventricular cells or none at all [20].

Taken together, this work will thoroughly assess the electrical properties and roles of T-tubules and a better fundamental understanding of T-tubules will contribute to a better understanding of the implications of T-tubular remodeling in disease.

2. T-tubules – the basics

2.1 T-tubules in cardiac excitability

The benchmark role of T-tubules is to facilitate excitation-contraction coupling [7], the process that couples the action potential with muscle contraction. The cardiac action potential is triggered when gap junctions at the intercalated disc, where two cardiomyocytes are connected [21], conduct a depolarizing current from an excited to a resting cell. Once the membrane potential reaches the activation threshold of voltage-gated sodium channels, these channels open quickly and conduct a large inward sodium current, further depolarizing the membrane (see **Fig. 2**). Sodium channels at the intercalated disc may also be activated by ephaptic interactions [22-24], a process relying on interactions between sodium current and extracellular potential. Besides the intercalated disc, sodium channels are also expressed in the lateral membrane [25]. Whether sodium channels are present in the T-tubules will be discussed in a later chapter. As soon as the membrane has depolarized further, the L-type voltage-gated calcium channels, which are mainly located in the T-tubules [26], also open and conduct an inward calcium current. Voltage-gated calcium channels are close to (~ 15 nm) ryanodine receptors (isoform RyR2 in the heart) in the sarcoplasmic reticulum (SR) [7], together forming dyads. Calcium influx through T-tubular channels therefore quickly leads to calcium efflux from the SR conducted by RyR2, a process called calcium-induced calcium release [7]. The increased intracellular calcium concentration then induces sarcomere shortening [7]. By bringing voltage-gated calcium channels close to sarcomeres at the periphery as well as in the core of the cell, T-tubules provide a large stage for calcium handling proteins, promoting synchronous contraction of the whole depth of the cell [27]. Later during the action potential, voltage-gated potassium channels also open. The opposing potassium and calcium currents create the plateau of the action potential, where the membrane stays depolarized for a while, after which calcium channels close and the potassium current repolarizes the sarcolemma. Then, the sodium-potassium ATPase and the sodium-calcium exchanger among others restore ion concentrations at both sides of the membrane, while SERCA (sarco/endoplasmic reticulum Ca^{2+} ATPase) takes up calcium from the myoplasm back into the SR.

T-tubules also serve as hubs for signaling molecules. Catecholamines for instance bind to β-adrenergic receptors in the T-tubules, modifying cardiac contraction and relaxation [6].

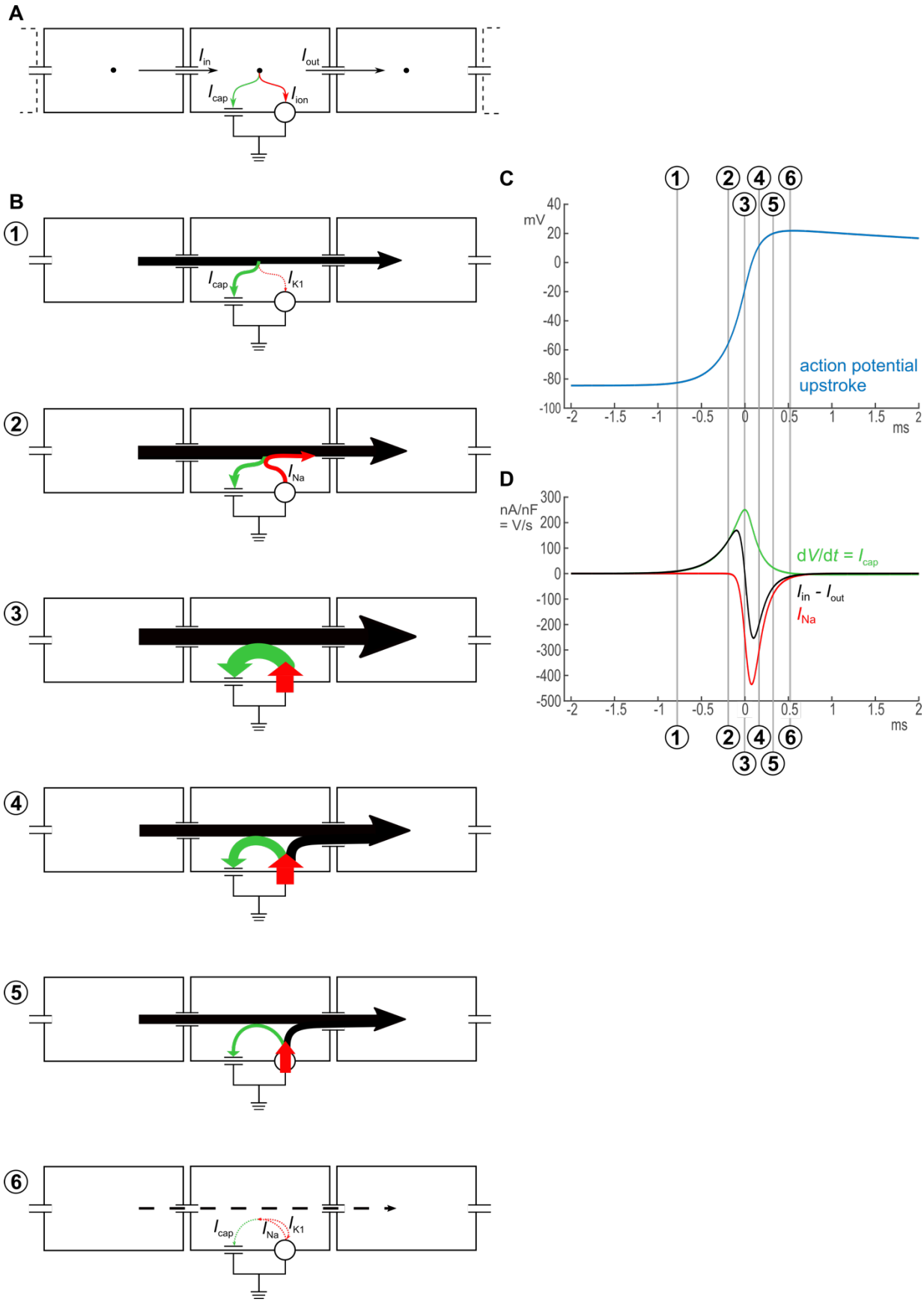
A
I_{in}
I_{out}
I_{cap}
I_{ion}
B
①
I_{cap}
I_{K1}
②
I_{Na}
③
④
⑤
⑥
I_{cap}
I_{Na}
I_{K1}
C
① ② ④ ⑥
③ ⑤
mV
40
20
0
-20
-40
-60
-80
-100
-2
-1.5
-1
-0.5
0
0.5
1
1.5
2
ms
action potential
upstroke
D
nA/nF
= V/s
300
200
100
0
-100
-200
-300
-400
-500
dV/dt = I_{cap}
I_{in} - I_{out}
I_{Na}
① ② ④ ⑥
③ ⑤

Figure 2. Principles of conduction and current flow during the upstroke of the action potential. Panel **(A)** depicts a strand of cardiac cells. During action potential propagation, current will enter a given cell through gap junctions at one end of the cell (I_{in}) and leave through gap junctions at the other end *(I_{out}).* The cell membrane is represented by a capacitance connected in parallel to all ion currents. The membrane current is thus the sum of the capacitive and ionic currents (I_{cap} and I_{ion}, respectively). Panel **(B)** describes currents in the middle cell at different stages (1-6) of the action potential upstroke, corresponding to numbers 1-6 in panels **(C)** and **(D)**. **Stage 1**: at the foot of the upstroke, a part of I_{in} will charge the membrane (I_{cap}, green), while a very small outward current (I_{K1} and I_{leak}, red) will leak through the membrane. I_{K1} and I_{leak} are very small and are not depicted in stages 2-5. **Stage 2**: a fraction of I_{in} is transferred to the membrane as I_{cap} while the first sodium channels open (red) and contribute to I_{out} and I_{cap}. **Stage 3**: at the time of dV/dt_{max}, I_{in} equals I_{out}. Therefore, at this time point, the large inward sodium current serves to depolarize the membrane. **Stage 4**: now, I_{out} is larger than I_{in}. The sodium current contributes to I_{out} as well as to I_{cap}. **Stage 5**: I_{in} further decreases. I_{Na} is also smaller, yet still contributes to I_{cap} and I_{out}. **Stage 6**: end of the upstroke. Most sodium channels are inactivated, very little current is flowing. Panel **(C)** and **(D)** depict the relationship between action potential upstroke and ion currents. **(C)** The blue curve represents the upstroke of the action potential. **(D)** The green curve depicts dV/dt, which reflects the capacitive current. The red curve represents the sodium current normalized to cell capacitance, which is at its maximum just after the dV/dt_{max}. Note that during the upstroke, the sodium current prevails largely over the other ion currents. The difference between current entering and exiting the cell (I_{in} - I_{out}), also normalized to cell capacitance, is given by the black curve. This curve is directly following the sum of capacitive and transmembrane ion currents (in this case, only the sodium current is relevant).

2.2 Structure

T-tubules can be subdivided in transversal tubules, perpendicular to the lateral sarcolemma and running along the z-discs of sarcomeres, and longitudinal or axial tubules that link transversal tubules to each other (**Fig. 1B**). T-tubules however do not form a continuous network throughout the cell. The mean length for a T-tubular segment in rats is about 6.8 μm [1]. Of note, T-tubular structure differs considerably between species. For instance, in sheep, axial segments make up 9% of total T-tubular volume, but 60% in rat [1]. Described T-tubular luminal diameters range from 20 to 450 nm, with an average of 200-300 nm in rat [1] (reviewed in [5]). For the sake of comparison, T-tubules of skeletal muscle are only 30 nm in diameter [28]. When considering cardiac T-tubular openings, those in rabbit are wider than in mouse [29]. As a rule, mammals with a high heart rate, such as mice, have a much denser T-tubular network with smaller diameters than low-heart rate species, such as human [3, 27]. Possibly, the higher the heart rate, the faster and more efficient excitation-contraction coupling must occur, and the more membrane surface is required to accommodate more calcium-handling structures such as dyads.

As for membrane area, the measurements differ depending on the applied method, even within one species. For rats, T-tubular membrane area estimations range from 21 to 64% of total sarcolemma [30]. Causes and implications of these differences will be discussed extensively in **Section 3.3**.

On a nanoscale, T-tubules connect with the flat ends of SR, known as terminal cisternae, where dyads are located. Connections of T-tubules with the nuclear envelope, endoplasmic reticulum (ER), and mitochondria have also been described [5, 31]. Nuclear envelope-T-tubule connections are likely to facilitate a process called excitation-translation coupling [32]. Moreover, the T-tubular membrane forms microfolds. Their folding is mediated by the BAR-domain protein Bin1 [33].

T-tubules also contain caveolae, 50-100 nm-wide flask-shaped invaginations of the membrane. Their coating of caveolin and cavin sets them apart from other lipid rafts. The density of caveolae seems to be equally high in the T-tubular and other sarcolemma [34, 35].

Considering that T-tubules associate with many proteins and have tortuous membrane folds, T-tubules are complex structures that still can be dynamic under certain circumstances, for instance in disease [9, 36].

2.3 Regulation and signaling

Many factors regulate T-tubules biochemically or biophysically, a few of which will be mentioned in this section (reviewed in [5, 6, 27]). Caveolae for instance compartmentalize specific signaling proteins, such as the β_2-adrenergic receptor (β_2-AR), which forms signaling clusters with the G protein G_s and G_i. G_s activates the adenylyl cyclases AC5 and AC6 and PKA. AC5 and AC6 in turn produce cAMP, which has a wide range of downstream effects. Targets of PKA include calcium-handling proteins such as the voltage-gated calcium channel and RyR2, and the sarcomeric proteins troponin I and C. β_1-AR on the other hand is not confined to caveolae and couples exclusively to the stimulatory G_s pathway (reviewed in [6]). The L-type voltage-gated calcium channel is expressed both inside and outside of caveolae. The caveolar channels appear to be cAMP-activated and affect hypertrophy instead of excitation-contraction coupling [37]. Other noteworthy regulators of T-tubules are: (1) Tcap, which regulates the formation of T-tubules under influence of load and stretch of the cell [38]; (2) junctophilin-2, which stabilizes dyads [39, 40]; and (3) Bin1, which folds the T-tubular membrane and recruits calcium channels [41, 42].

3. Electrical properties of T-tubules

3.1 Passive properties

In this section, we will address the electrical properties of T-tubules, and how they affect cardiomyocyte excitability.

During the propagation of the depolarizing wavefront, the voltage difference between neighboring cells is the driving force for intercellular current. This current is conducted by gap junctions and depolarizes the

membrane of the neighboring cell. Once a membrane depolarizes at the surface of a myocyte, the change in voltage induces passive electrotonic responses of the T-tubular membrane for which ion channel openings are not required. To assess whether passive conduction suffices to depolarize the entire T-tubular system, cable theory comes into play [43, 44]. If we consider a passive T-tubular membrane, when the cell is excited by an action potential, the T-tubular transmembrane voltage drops due to current leaking across the membrane resistance (r_m) and flowing outwards down the T-tubules through their longitudinal resistance (r_{TT}). These effects limit the extent of electrotonic responses. To assess the decay of action potential propagation, the length constant for guinea pig T-tubules was theoretically estimated at $\lambda = 240$ μm [10, 45]. Kong *et al.* also calculated the length constant based on optical measurements in mouse cardiomyocytes at $\lambda \approx 240$ μm [46].

To assess passive electrical properties experimentally, Scardigli *et al*. [47] were inspired by an experimental geology study, in which conductivity of a porous rock was determined to assess the diffusive properties. In isolated cardiomyocytes, the apparent diffusion coefficient *D'* of fluorescent dextran was determined by fluorescence recovery after photobleaching (FRAP) microscopy. The cardiomyocytes were modeled as porous cylinders and Fick's second law of diffusion was applied to calculate *D'* from the time to recovery after photobleaching and the cellular radius ($D' \approx 1.4$ μm^2·s^{-1}). Based on the analogies between Fick's first law of diffusion and the electrical current density law, the electrical conductivity of T-tubules was determined at $K' = (5.3 \pm 0.5)\ 10^{-4}$ Ω^{-1}·cm^{-1}. Lastly, the length constant was calculated from the diffusion rate and the previously measured T-tubular surface area per unit cell volume: $\lambda = 290 \pm 90$ μm. This is very similar to the aforementioned values.

Scardigli *et al.* however did not properly consider that the analogy between conductivity and diffusion depends on the detailed porous structure, which in geology is described by the so-called "formation factor". This factor describes the ratio of the resistivity of a porous rock filled with water to the resistivity of water and must be empirically measured or defined for different rock types. For cardiac myocytes, the actual factor is unknown. Scardigli *et al.*'s estimate of the diffusion coefficient may therefore be subject to uncertainty and thus differ from values reported by for instance Kong *et al.* ($D' \approx 23$ μm^2·s^{-1}) [29]. The obtained length constant however resembled that found by Kong *et al*. because the formation factor offsets diffusion [29].

For a rat T-tubule with a mean length of 6.84 μm [1], Scardigli *et al.* calculated a voltage drop from the surface sarcolemma to the cell core of ~ -4 mV assuming an infinite cable, and thus an exponential decay of potential along the T-tubule. The voltage drop in an infinite cable can be described by [48, 49]

$$\Delta V(x) = \Delta V_0 \left(e^{-\frac{x}{\lambda}}\right), \quad \text{(Eq. 1)}$$

where ΔV_0 = 100 mV and λ is the length constant, which can be described by the following cable-theory-derived equation [49]

$$\lambda = \sqrt{\frac{r}{2 g_{\mathrm{m}} \rho_{\mathrm{e}}}} \quad \text{(Eq. 2)}$$

where r is the T-tubular lumen radius, g_{m} the conductance of resting membrane per unit area, and ρ_{e} the resistivity of extracellular space. A sealed-end cable however approaches a T-tubule more closely than an infinite cable does. Voltage drop in a sealed-end cable at depth x can be described by [48, 49]

$$\Delta V(x) = \Delta V_0 \, \frac{\cosh\left(\frac{L-x}{\lambda}\right)}{\cosh\left(L/\lambda\right)}, \quad \text{(Eq. 3)}$$

where L is the T-tubule length [48]. **Eq. 3** decreases less steeply with x than **Eq. 1**, and if $L \ll \lambda$, $\Delta V(x)$ hardly decays at all as described by **Eq. 3**. For the T-tubular properties described by Scardigli, **Eq. 3** yields a much smaller voltage drop of -0.028 mV [50].

Uchida and Lopatin [51] recently showed that a length constant of ~ 290 µm is probably a significant overestimation, because the previously discussed publications [45, 47] did not take the dilations and constrictions of T-tubules into account. In addition, T-tubules form branching networks, and can also form loops. In neuroscience, much effort was invested in deriving simplifying formulas to describe the decay of the electrotonic potential in neuritic trees with changing neurite diameters (e.g., flaring, tapering) and branches [49, 52-55]. For example, Rall has shown that a branching dendritic tree can be collapsed to a cylinder model under certain stringent constraints such as defined relationships between the diameters of parent and daughter branches [54-56]. While certain neurons may exhibit parent and daughter branch diameters compatible with such constraints, these constraints certainly do not pertain to T-tubules. The morphological heterogeneity of T-tubules disqualifies the straightforward application of classic cable theory.

Uchida and Lopatin determined the diffusion coefficient $D'_{\mathrm{TT}} \approx 4$ µm^2·s^{-1} in murine cardiomyocytes. This is comparable to the findings of Scardigli *et al.* ($D'_{\mathrm{TT}} \approx 1.4$ µm^2·s^{-1} as mentioned previously) [47], but not to the findings from Kong *et al.* who calculate a much higher diffusion coefficient in murine T-tubules of ~ 23 µm^2·s^{-1} for 1 kDa solutes [29]. The diffusion coefficient found by Kong *et al.* corresponds to a ~ 12 times reduction of free diffusion rate, which is comparable to the ~ 8 times reduction of calcium ion diffusion estimated based on electrophysiological experiments [57]. This finding from Kong *et al.* likely approximates the *in vivo* diffusion coefficient better since their model is not confounded by cell and illumination beam geometries, which might have affected the results from Scardigli and Uchida [47, 51]. Interestingly, the diffusion coefficient in rabbit T-tubules is only ~ 5 times slower than free diffusion rate

compared to the ~ 12 times reduction in mice [29]. This difference can be explained by the structural differences between murine and rabbit T-tubules: murine T-tubules are more tortuous close to the surface than rabbit T-tubules, and the luminal "ground substance" identified by electron microscopy – potentially representing the glycocalyx – forms a stronger diffusion barrier in murine T-tubules [29].

Uchida and Lopatin furthermore illustrate the importance of T-tubular structure in determining the diffusion time [51]. The *in vivo* diffusion time constant of 3.9 s could only be approached in an *in silico* 3D cell model of murine T-tubules by introducing 20-nm-wide constrictions and 600-nm-wide dilations in the model (values represent luminal diameters; $\tau_{dilations}$ = 2.2 s and $\tau_{constrictions}$ = 2.5 s) [51]. Extrapolating this to electrical properties under standard conditions for specific membrane capacitance, extracellular and membrane resistivity, the time constant for cylindrical T-tubules would be τ_{Vm} = 10.1 μs and for T-tubules with dilations or constrictions τ_{Vm} = 102 μs [51]. The latter time constant approaches the experimental finding $\tau_{Vm} \approx$ 200 μs in murine T-tubules [58]. Uchida and Lopatin however do not consider microfolds [33]. This membrane tortuosity could be corrected for by increasing the specific capacitance from 1 to 2 μF/cm^2, which would double the time constant τ_{Vm} from ~ 100 μs to ~ 200 μs, which is even closer to the experimental finding [58].

Constrictions and dilations considerably affect the length constant. For a 200-nm-wide T-tubule with short 20-nm-wide constrictions every 2 μm, $\lambda_{TT} \approx$ 68 μm [51]. This is considerably smaller than the $\lambda_{TT} \approx$ 240-290 μm reported before [45, 47]. To transition from the steady state to the non-steady state, the length constant needs to be corrected for the characteristic frequencies (f) of the action potential (during the upstroke, $f \approx$ 150 Hz) [46], and λ_{AP} will be ~ 34 μm [51]. Since the length constant also depends on membrane resistance R_m, the length constant will decrease further when voltage-channels are open.

This implies that, in an average murine T-tubule of 9 μm long [42], the voltage drop will be ~ -13 mV from the surface to the end of the T-tubule when assuming an infinite cable as described by **Eq. 1**. When assuming a sealed-end cable, the applicable equation is **Eq. 3**, which gives a voltage drop of only 0.87 mV. In any case, this voltage drop is small enough to allow voltage-gated calcium channels to open, assuming that the surface sarcolemma depolarizes to +20 mV and the threshold of calcium channels lies near -40 mV. The question whether the entire T-tubular membrane depolarizes quickly enough to open calcium channels once a cell is excited is discussed in **Section 3.2**. To conclude, we have to keep in mind that passive electrical parameters will differ significantly between species. Whereas rabbit T-tubules openings are relatively accessible and easy to follow, openings of murine T-tubules are relatively tortuous and filled with glycocalyx, which considerably limits diffusion [29].

3.2 Delay of T-tubular membrane depolarization

T-tubules greatly increase membrane surface, so charging the capacitance of the membrane of a tubulated cell will take longer. The time it takes to charge the membrane as a capacitor and depolarize T-tubules was assumed to be negligible [45, 59], but recent results indicate this is incorrect [50, 60]. Quantifying the capacitance charging time of T-tubules would give important insight into the delay between the opening of voltage-gated channels at the sarcolemma and those deep in the T-tubules. This section addresses this depolarization delay and the effect of voltage-gated sodium channels on tubular depolarization.

We developed a simple computational model of a murine T-tubule, represented as a 9-µm-long cylinder with a diameter of 98.5 nm and a specific capacitance of 2 µF/cm^2 to simulate microfolds (normal specific capacitance is considered 1 µF/cm^2), subdivided in 100 segments. This model revealed a depolarization delay of 10 µs in the innermost segment in the absence of inward currents in the T-tubules [50]. This value is expected to greatly increase in the presence of T-tubular branches and frequent 20-nm-diameter constrictions. Conversely, sodium currents may facilitate T-tubular depolarization. Although Uchida and Lopatin determined that these structural changes increase the time constant of depolarization from ~ 10 to ~ 100 µs for this model (see **Section 3.1**) [51], they did not determine the delay of membrane depolarization of a deep T-tubular segment. Of note, linear cable theory assuming a passive linear membrane has limited applicability to a T-tubule given their non-linear current-voltage relationships. It is expected that the depolarization delay of a deep segment of a T-tubule with constrictions and dilatation is considerably greater than the 10-fold increase by which the time constant increased, because each dilatation poses a large capacitive load, in addition to the depolarization delay due to the higher resistance in each constriction. Taken together, the question remains open how much later voltage-gated calcium channels open deep inside the T-tubules when the surface sarcolemma is excited.

The effect of a voltage-gated sodium current on the depolarization of T-tubules and the effects of intratubular potentials on the sodium current have been simulated by Hatano *et al*. [60] in an elaborate 3D model with structurally simple T-tubules without branches, constrictions and dilations. The T-tubular sodium current density was set at 30 mS/µF according to experimental results from [45] (see **Section 3.4.2** for a critical evaluation of these results). In the deepest segments of the modelled T-tubule (5 µm from the surface), the extracellular potential was slightly negative (-1 mV) because of the flow of current along the narrow tubule. Due to this negative potential, the sodium current was ~ 8% smaller in the deep segment than the segment at the cell surface [60]. A similar result was obtained with our simpler model [50] with a slightly smaller T-tubular sodium current density of 23 mS/µF. The mechanism underlying this sodium current reduction in the deep portions of the T-tubules resides in the notion that an ion current I_X carried by ion species X can be described by $I_X = g_X \cdot P_O \cdot (V_m - E_X)$, where g_X is the maximal conductance of that

current, P_O is the open probability of the corresponding channels, V_m is membrane potential, and E_X is the reversal potential of I_X. The term V_m - E_X is called the driving force. For the case of the sodium current, the driving force becomes smaller (in absolute value) when the extracellular potential becomes negative, thus decreasing the current (in absolute value). A comparable mechanismwas called "self-attenuation", and has been proposed to occur in intercalated discs due to ephaptic interactions [22-24]. Thus, the sodium current is slightly self-attenuating deep inside the T-tubules. Additionally, the tubular lumen can be transiently depleted from sodium if the T-tubular sodium current is substantial. Sodium depletion decreases E_{Na}, the Nernst potential of sodium and thus the driving force, representing an additional mechanism reducing the sodium current. This was specifically addressed in a modeling study by Mori *et al.* who showed that sodium depletion in the intercalated disc contributes to self-attenuation [61]. In addition, a recent study by Greer-Short *et al.* indicates that sodium depletion in intercalated discs and the resulting decreased driving force for sodium ions are also important in shaping repolarization as they attenuate the late sodium current. Interestingly, this phenomenon can mask the phenotype of long-QT syndrome type 3 [62].

3.3 Influence of T-tubules on macroscopic conduction velocity

In this chapter, we will assess theoretically how macroscopic conduction velocity (i.e., conduction along the surface membrane and throughout cardiac tissue) is influenced by T-tubular ion channels and membrane. To do so, one has to take a closer look at the propagation of action potentials through cardiac tissue. Much insight has been gained from the ground-breaking work of Hodgkin and Huxley and others [12-16, 63].

Firstly, one has to understand the dynamics of current flow into, out of, and within a cell during the propagation of the depolarizing wavefront as detailed and illustrated in **Fig. 2**. The dynamics of various currents during the upstroke of the action potential are crucial determinants of conduction.

During the passage of a wavefront, electrotonic current enters the cell from upstream (I_{in}) and exits the cell downstream (I_{out}) (**Fig. 2B** and **2D**, in black). According to Kirchhof's current law [64], the difference I_{in} - I_{out} must be transferred to the membrane in the form of capacitive current (I_{cap}; **Fig. 2B** and **2D**, in green) or flow through membrane ion channels and transporters (I_{ion}; **Fig. 2B** and **2D**, in red).

The capacitive current I_{cap} directly follows the upstroke velocity of the action potential (**Fig. 2C**), i.e., the rate of change of membrane potential V, expressed as $\partial V/\partial t$. Assuming that cell capacitance C is constant, I_{cap} is indeed defined as:

$$I_{\text{cap}} = C \cdot \frac{\partial V}{\partial t}. \quad \text{(Eq. 4)}$$

Thus,

$$I_{\text{in}} - I_{\text{out}} = C \frac{\partial V}{\partial t} + I_{\text{ion}}. \quad \text{(Eq. 5)}$$

Assuming that the cell is much smaller than the length constant of the tissue and the spatial extent of the upstroke (which is the case for well-coupled cardiac tissue), then the tissue can be considered as a continuous syncytium [17, 64]. In one dimension, **Eqs. 4** and **5** can be written in a spatially continuous form as:

$$\sigma \frac{\partial^2 V}{\partial x^2} = c \frac{\partial V}{\partial t} + i_{\text{ion}}, \quad \text{(Eq. 6)}$$

where x is position, σ is the lumped conductivity (normalized by surface-to-volume ratio) of the gap junctions, the intracellular space, and the extracellular space; c is the membrane capacitance per unit area; and i_{ion} is the total ion current per unit area. This equation is known as the cable equation [12, 13], or in the cardiac community as the monodomain equation, which is valid for cardiac tissue when assuming that the anisotropy ratios of intra- and extracellular resistivities are equal [64].

When conductivity (σ) changes, conduction velocity (θ) follows a square-root relationship [13, 49, 64]:

$$\theta \propto \sigma^{1/2}. \quad \text{(Eq. 7)}$$

Now, we will consider three possible scenarios to assess the influence of T-tubular membrane and channels on conduction (**Fig. 3**). In the first (**Fig. 3A**), T-tubules contain a low density of channels, especially of voltage-gated sodium (Na_v) channels (or an absence of Na_v channels in the extreme case). In the second scenario (**Fig. 3B**), we will consider that the composition of Na_v channels in the T-tubular membrane is the same as in the surface sarcolemma. In the third (**Fig. 3C**), we will consider that the density of Na_v channels is higher in the T-tubular membrane than in surface sarcolemma. We initially assume that the axial resistance of the T-tubules and the intratubular potential gradient are negligible. This is equivalent to assuming a homogeneous membrane potential throughout the cell surface and T-tubular membranes. Thus, we assume that the T-tubular membrane potential quickly follows the lateral membrane potential, and that extracellular potentials in the T-tubular lumen are small [50, 60]. These three scenarios therefore correspond to changing the total capacitance and/or the number of channels in the membrane.

The first scenario (few or no Na_v channels in the T-tubules, **Fig. 3A**) corresponds to scaling the specific membrane capacitance c in the cable equation (**Eq. 6**). Intuitively, adding capacitance would increase the load to excite the tissue and slow conduction. This scenario is however difficult to assess theoretically in a

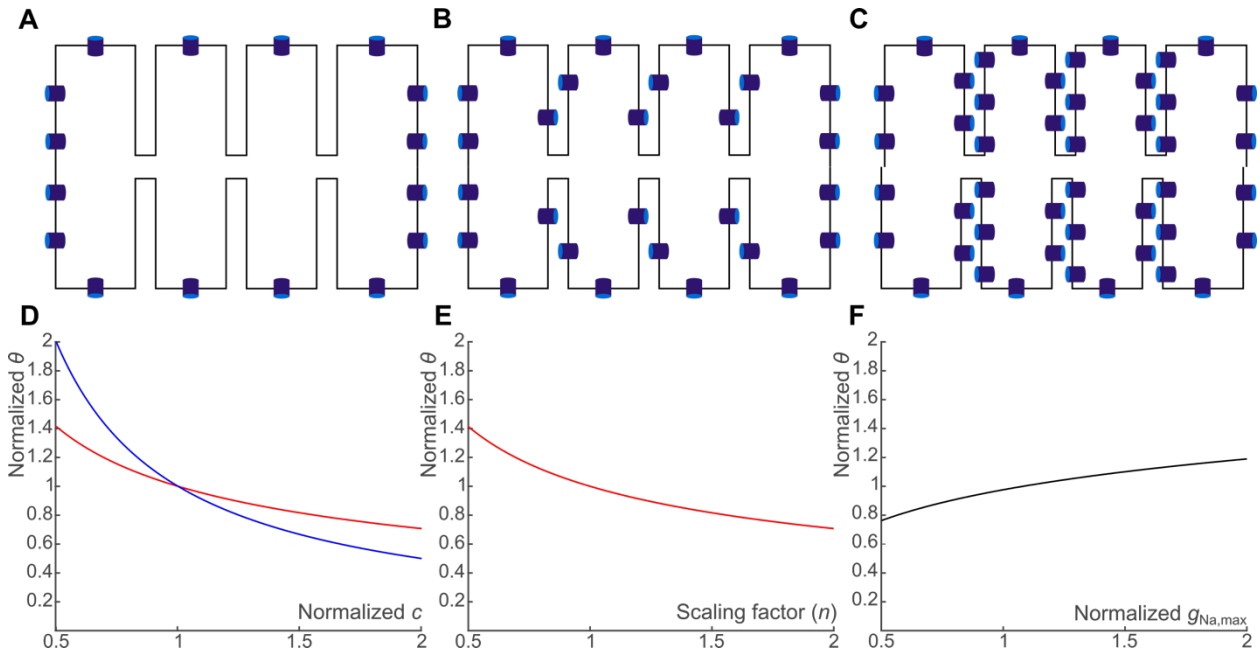

Figure 3. Scenarios in assessing the influence of T-tubule composition on macroscopic conduction velocity (along the surface membrane and throughout cardiac tissue). **(A)** First scenario: T-tubules contain no (or very few) voltage-gated sodium channels. **(B)** Second scenario: density of voltage-gated sodium channels is similar inside and outside of T-tubules. **(C)** Third scenario: T-tubules contain a higher voltage-gated sodium channel density than surface sarcolemma. **(D)** Relationship (pertaining to the first scenario, **A**) between normalized conduction velocity (θ) and normalized capacitance (c) as defined by inverse square root (red) and inverse (blue) functions, corresponding to Eqs. 8 and 9, respectively. **(E)** Relationship (pertaining to the second scenario, **B**) between normalized θ and the scaling factor n, described by the inverse square root function corresponding to Eq. 10. **(F)** Relationship (pertaining to the third scenario, **C**) between normalized θ and the normalized $g_{Na,max}$ as described by the logarithmic dependence given in Eq. 11, with $k = 0.308$.

quantitative manner. It is reminiscent of myofibroblasts connected to myocytes with a high level of gap junctional coupling, although myofibroblasts will render the resting membrane potential of the myocytes less negative. The effects of such an additional capacitive load have been studied by Jacquemet and Henriquez [65].

Huxley [66] as well as Jack, Noble and Tsien [49] have addressed our first scenario theoretically in detail, and showed that the kinetic properties of the voltage-gated ion currents also determine the exact relationship between conduction velocity (θ) and capacitance (c). Nevertheless, θ is expected to decrease when c increases. The relationship between θ and c lies between

$$\theta \propto c^{-1/2}. \quad \text{(Eq. 8)}$$

and

$$\theta \propto c^{-1}. \quad \text{(Eq. 9).}$$

These relationships are illustrated in **Fig. 3D**. Thus, in the extreme case of this first scenario and assuming that T-tubules contribute 50% to cell capacitance, θ may be decreased by an amount between 29% (**Eq. 8**) and 50% (**Eq. 9**).

The second scenario (same ion channel composition of the T-tubular membrane as the surface sarcolemma; **Fig. 3B**) corresponds to changing I_{ion} and I_{cap} by the same factor. If the two summands of the right hand side of the cable equation (**Eq. 6**) are scaled by a factor n, we can observe that the cable equation remains the same if σ is also scaled by n. Thus, in terms of effects on θ, scaling I_{ion} and I_{cap} by n is equivalent to scaling σ by $1/n$ and we can expect that θ will behave as

$$\theta \propto n^{-1/2}. \quad \text{(Eq. 10)}$$

Therefore, if T-tubules contribute 50% to cell capacitance, θ may be decreased by up to 29% (**Fig. 3E**).

Finally, the third scenario corresponds to adding relatively more Na_v channels than membrane (**Fig. 3C**). In the extreme situation of adding Na_v channels only, θ is expected to increase [63]. In a computer model of conduction, King and Fraser [44] have shown empirically that θ is linearly related to the logarithm of $g_{Na,max}$, i.e.,

$$\frac{\theta}{\theta_{ref}} = 1 + k \log\left(\frac{g_{Na,max}}{g_{Na,max,ref}}\right) \quad \text{(Eq. 11)}$$

where θ_{ref} is the reference control velocity, $g_{Na,max}$ is the maximal conductance of Na_v channels, $g_{Na,max,ref}$ is the reference control $g_{Na,max}$, and k is a model-dependent constant that must be determined empirically. For conduction in the Luo-Rudy dynamic model as investigated by Shaw and Rudy [63], we estimated k to be 0.308. The function given by **Eq. 11** is illustrated in **Fig. 3F**. Thus, θ may increase due to the larger Na_v channel density, but this effect may be opposed by the increase of c. The net effect will depend on the exact change of $g_{Na,max}$ and c. This scenario however appears unlikely in the light of recent experimental data, since studies addressing Na_v expression in the T-tubules have suggested that at most 29% of Na_v channels are present in the T-tubules [67], which may be an overestimation (see **Section 3.4.2** for a detailed discussion).

Next, we conjecture about the additional effects of T-tubular exit resistance and associated large T-tubular potential gradients on macroscopic conduction velocity (along the surface membrane and throughout cardiac tissue). On the one hand, a substantial exit resistance would tend to decouple the capacitive load of the T-tubules, thereby accelerating macroscopic conduction. In the limit of a very large resistance, the load of the T-tubules would be fully decoupled, corresponding to a detubulated situation. However, the experimentally observed time constants in the range of 100-200 µs [51, 58] and the small potential gradients

reported in modeling studies [50, 60] suggest that the exit resistance is small. The reported time constants of 100-200 μs are moreover much shorter than the typical timescale of the upstroke of the action potential (~ 1 ms), suggesting that the capacitive load only has small effects on the action potential upstroke. These considerations are in line with those of Jacquemet and Henriquez [65], who studied the effects of the capacitive load of fibroblasts in various myocyte-fibroblast coupling regimes. Of note, a large exit resistance would slow conduction along the T-tubules.

On the other hand, we note that the exit resistance of the T-tubules will directly influence the level of self-attenuation. If the exit resistance is small, self-attenuation will be negligible, and we expect no influence on conduction velocity. If the exit resistance is sufficiently large, self-attenuation of the sodium current will appear because of the large negative tubular potential, which would tend to slow conduction. Current results of computer simulations suggest that self-attenuation is in the range of a few percent [50, 60], and the resulting conduction slowing would also be in the percent range. An increase in the tubular resistance would however also decrease the capacitive load (see above), which may compensate the conduction slowing. In the extreme case of a very large exit resistance, we would retrieve once more the detubulated situation. Since there is no experimental proof of sodium current self-attenuation in the T-tubules for the moment, we must limit ourselves to speculation.

In summary, the reality most likely lies somewhere between the first two scenarios, so the presence of T-tubules will decrease θ. Conversely, loss of T-tubules may accelerate conduction. To explicitly investigate all these factors, including T-tubule resistance, intratubular potential gradients, and self-attenuation of the sodium current, specific modeling approaches need to be developed.

3.4 Action potentials in T-tubules?

A logical follow-up question to the passive conductive properties of T-tubules is: are action potentials generated in T-tubules? To generate an action potential, the right collection of depolarizing currents (conducted by voltage-gated sodium and calcium channels) and repolarizing current (conducted by potassium channels) must be present. This section discusses evidence regarding the presence or absence of ion channels in the T-tubules.

Firstly, it must be noted that data regarding T-tubular action potentials and ion channel expression require careful interpretation. In functional experiments, the cell capacitance is used to calculate membrane surface area, often assuming that 1 μF corresponds to 1 cm^2 membrane area [35]; thus, dividing whole-cell current by capacitance gives current density. Any difference in current density between normal and detubulated cells should indicate that the density of ion channels differs between T-tubular and non-T-tubular

sarcolemma [26, 67]. A caveat of this assumption is that measuring the capacitance underestimates the T-tubular membrane surface, since optical measurements give much higher fractions of T-tubular membrane (65% versus 32% from capacitance-based measurements [30]). One partial explanation for this discrepancy is the fact that capacitance is often determined too straightforwardly when the current transient evoked by a voltage-clamp step is simply integrated and divided by the commanded voltage step [68]. This method underestimates the capacitance if the opening of the cell at the pipette is imperfect, yielding a higher access resistance and a concomitant increase in capacitance charging time, and if the cell cannot be approximated as a single resistance in parallel with a single capacitor, which is the case for structurally complex cells such as cardiomyocytes. As a result, the apparent time constant of the current transient charging the capacitor increases, and from a certain time constant value, the "tail" of the current transient is usually excluded from the integration. The resistance that certain structural obstacles pose to the capacitive current may moreover be so high that the membrane depolarizes too late for the ion channels in this region to be activated. The ability to depolarize the entire cell membrane on a satisfactorily short time scale is called space clamp. In other words, in a voltage-clamped cell, the transmembrane potentials will differ between different portions of the membrane due to electric field interactions with geometric barriers.

Taken together, these pitfalls lead to an underestimation of membrane area of normal (non-detubulated) cells and an overestimation of current density. Therefore, the fraction of T-tubular current density must be lower than the capacitance-based measurements implicate, and ion channel density in T-tubules will be overestimated.

Indeed, when ion channel densities are determined from functional experiments, only rarely the results are corrected for cell surface [30]. Pásek *et al.* [30] reconcile the discrepancy between membrane area estimations by assuming a lower specific capacitance of T-tubules due to the relatively high cholesterol concentration in T-tubular membranes, and correcting for incomplete detubulation, setting T-tubular membrane surface at 49% instead of 32%. This reconciliation should lead to a decrease in current attributed to the T-tubules, even after correcting for the fact that formamide treatment leaves about 7% of T-tubules unaffected. A recent study however invalidated the hypothesis that cholesterol reduces the specific capacitance [69]. The discrepancy between electrophysiological and optical surface measurements may also be sought in difficulties in obtaining a complete space clamp in cardiomyocytes.

Comparing currents between whole-cell and detubulated cells may be complicated by more factors. Firstly, applying an osmotic shock to a cell may elicit unwanted effects which have not yet been investigated. The sudden internalization of membrane proteins may result in other acute membrane remodeling responses; the remodeling of structural proteins may affect protein expression at the membrane. Secondly, the sodium current in deep T-tubular segments may self-attenuate (see **Section 3.2**) [50, 60], so whole-cell peak sodium

current may not reflect the full available sodium current. Taken together, it is crucial to keep in mind that ion current densities between normal and detubulated cardiomyocytes should not be compared without taking into account the limitations mentioned above.

Immunohistochemistry data also require careful interpretation. Ideally, any staining for T-tubular proteins should be combined with a fiducial T-tubular marker and a knock-out model to assess the specificity of the antibody. Most publications addressing ion channel expression in T-tubules miss one or both of these quality controls. As a good example, Eichel *et al.* [70] show that the staining for the ion channel regulator CASK follows a regular striated pattern in cardiomyocytes, which may indicate T-tubular localization. The signal however did not colocalize with RyR2 and $Ca_v1.2$, so the authors concluded that CASK was not expressed at the T-tubules [70]. We will therefore interpret published data on ion channel expression in T-tubules carefully.

3.4.1 Calcium-handling proteins

The **voltage-gated calcium channel** consists of an α-subunit with multiple auxiliary β-, $\alpha_2\delta$- and γ-subunits [71]. The predominant cardiac splice variant of the α-subunit is $Ca_v1.2$ (reviewed in [5]). Electrophysiological studies in detubulated and normal rat cardiomyocytes have determined that 60-75% of calcium current is conducted by calcium channels in the T-tubules [26, 72]. The authors did not normalize the calcium influx [26] or whole-cell calcium peak current [72] to the cell capacitance; the difference in calcium influx or peak current between control and detubulated cardiomyocytes already indicated which fraction of calcium channels was localized in the T-tubules. The previously stated problems with normalizing whole-cell currents by capacitance (**Section 3.4**) do therefore not apply to these studies.

Most calcium channels in the T-tubular membrane are close (~ 15 nm) to RyR2 in the SR, forming dyads [73]. This close proximity allows calcium ions entering the cell through $Ca_v1.2$ to quickly and efficiently bind RyR2, followed by calcium-induced calcium release from the SR and subsequent sarcomere shortening. RyR2 and $Ca_v1.2$ stay so close together because junctophilin-2 bridges the membranes of the SR and T-tubule to stabilize the dyad [39]. RyR2 and $Ca_v1.2$ both bind Bin1, a banana-shaped protein that assists in trafficking and clustering of calcium channels [41].

The **sodium-calcium exchanger NCX** is predominantly expressed in the T-tubules. With detubulation experiments in rat cardiomyocytes, 60% of total NCX current – both outward an inward – was determined to originate from the T-tubules, corresponding to a ratio NCX current carried by the T-tubules/surface membrane of 1.5 [74]. Another study stated on the basis of similar detubulation experiments that the ratio of NCX-carried current in T-tubular to that carried in surface membrane varies from 1.7 to 25 [75]. Both

aforementioned publications determine T-tubular NCX currents by comparing current densities, which methodological problems have been outlined extensively in **Section 3.4**. It is therefore likely that T-tubular NCX currents make up less than 60% of total. When we assume that T-tubules account for 50% of membrane surface [30], while the T-tubular membrane surface measured in [74] only was 32% of total, the T-tubular NCX current may be overestimated twofold. In other words, T-tubular NCX current may make up 30% rather than 60% of total current. Still, this does not necessarily conflict with the generally accepted idea that NCX plays an important role in calcium handling in T-tubules.

T-tubular NCX expression correlates with the function of T-tubules as the main stage for calcium handling: a relatively high concentration of $Ca_v1.2$ and RyR2 at the T-tubules facilitates a higher calcium conduction at the T-tubules than at the surface sarcolemma. This also requires more NCX activity to remove cytoplasmic calcium again. Indeed, NCX seems to be close to dyads, as well as SERCA, which pumps calcium ions back into the SR (reviewed in [27]), facilitating fast contraction as well as fast relaxation of the sarcomeres. $Ca_v1.2$ and the NCX isoform NCX1 are both reported inside and outside of caveolae [37, 76]. Dyadic $Ca_v1.2$ and NCX1 however most likely occur outside of caveolae, since caveolar $Ca_v1.2$ seems to play a role in the hypertrophy pathway and not to participate in contraction [37].

Ca^{2+} ATPase also extrudes calcium ions from the cytoplasm. Its activity is reported to be confined to the T-tubules in rat cardiomyocytes based on recordings in cardiomyocytes with the Ca^{2+} ATPase blocker carboxyeosin [77].

3.4.2 Sodium-handling proteins

The cardiac voltage-gated sodium channel **$Na_v1.5$** is crucial for generating the rapid upstroke of the action potential in cardiac cells. It is the first channel to open when the membrane depolarizes. It is unclear whether voltage-gated sodium channels are required in T-tubules, since the T-tubular membrane will depolarize quickly due to passive conduction alone, yet T-tubular Na_v channels would support conduction (see **Section 3.3**). Data regarding T-tubular sodium channel expression are multi-interpretable or inconclusive. Brette *et al.* concluded that 29% of sodium current is present in T-tubules because sodium current density in detubulated cardiomyocytes and normal cells were similar while cell capacitance decreased by 29% after detubulation [67]. After correcting for the larger T-tubular membrane area in untreated cells, however, current density would decrease. As a result, the calculated T-tubular sodium current fraction would be lower. We may also conclude that T-tubules do not contain Na_v channels because the same study showed that whole-cell sodium current did not differ between normal and detubulated cells [67].

When we consider immunohistochemistry data for $Na_v1.5$, we have to conclude that a reliable co-staining of $Na_v1.5$ and a T-tubular marker is still missing. Only a striated pattern of $Na_v1.5$ has supported the in our view premature conclusion that $Na_v1.5$ would be expressed in T-tubules [78-80].

Although $Na_v1.5$ is the main cardiac isoform of the voltage-gated sodium channel family, other isoforms have been reported in the heart [81]. It is important to keep in mind however that the expression of neuronal isoforms remains controversial. A recent report reported only $Na_v1.5$ and $Na_v1.4$ expression using next-generation RNA sequencing data from murine cardiomyocytes [82], yet other reports suggest that the neuronal isoforms $Na_v1.1$, $Na_v1.3$ and $Na_v1.6$ may be enriched in T-tubules [83-85] and even contribute to arrhythmias [86]. These neuronal channels have a lower activation threshold and inactivate more rapidly, which may facilitate action potential propagation into the T-tubules [5] – yet the fast passive propagation of depolarization renders T-tubular sodium channels relatively unessential. The immunohistochemistry data showing $Na_v1.1$, -1.3, and -1.6 in T-tubules of murine cardiomyocytes need careful interpretation because no knock-out control is presented for the antibodies [84, 86]. Another publication presents striated patterns of neuronal isoforms in immunohistochemistry data [85], whereas pre-absorbing the antibodies with peptides inhibits any staining, suggesting specificity of the antibodies [85]. Westenbroek *et al.* quantified the relative expression of $Na_v1.1$-6 in murine cardiomyocytes [87]. $Na_v1.5$ was only found at the intercalated disc and lateral membrane. $Na_v1.1$ and -1.3 showed a striated pattern, but compared to $Na_v1.5$, the signal intensity was relatively low, as was expected from protein expression data [88]. A T-tubular marker was however missing [87].

On a functional level, current conducted by neuronal channels was recorded in murine ventricular cardiomyocytes treated with β-scorpion toxin, a specific activator of neuronal sodium channels [85]. $Na_v1.6$-deficient mice moreover showed prolonged calcium transients in cardiomyocytes, suggesting a functional link between $Na_v1.6$ and excitation-contraction coupling [89]. In wild type mice, $Na_v1.6$ staining showed a striated pattern that weakly colocalized with α-actinin, but we have to consider that α-actinin is not an ideal T-tubular marker. $Na_v1.6$-deficient mice did not show any striated pattern, which suggests the anti-$Na_v1.6$ antibody binds specifically. In a model for CPVT (catecholaminergic polymorphic ventricular tachycardia), an arrhythmic persistent sodium current seemed to be conducted by neuronal Na_v isoforms [90]. The immunofluorescence data from this paper however show too high background signals to allow any conclusions on Na_v isoform expression.

Taken together, despite many reports on the expression of sodium channels in T-tubules, T-tubular Na_v expression remains debatable. A *de facto* inward sodium current by NCX should be expected in any case because of the high electrochemical gradient.

Lastly, **NKA** is expressed in T-tubules [91]. Especially the α_3-subunit is enriched in T-tubules, whereas the α_1-subunit is more uniformly expressed over the sarcolemma [91].

3.4.3 Potassium-handling proteins

Although the subcellular localization of potassium channels is less studied, several potassium currents seem to be conducted in the T-tubular systems of mice and rats. These include the inward rectifier current I_{K1} [58] (conducted by $K_{ir}2.1$, 2.2, and/or 2.3), the steady-state current I_{ss} ($K_v1.2$ and/or -2.1), the transient outward current I_{to} ($K_v4.2$ and/or -4.3), the slow delayed rectifier current $I_{K,s}$ ($K_v7.1$), and the rapid delayed rectifier current $I_{K,r}$ ($K_v11.1$/hERG) [30]. Based on detubulation experiments, I_{K1}, I_{to}, $I_{K,r}$, and $I_{K,s}$ seem to be divided equally over T-tubular and surface sarcolemma [92]. The inward-rectifying current I_{K1} is especially high in T-tubules because potassium accumulates in the small extracellular space during the repolarization phase of the action potential, increasing its driving force [58]. Other currents were found to be enriched in rat T-tubules, including I_{ss} [92]. Interestingly, only $K_v2.1$-encoding mRNAs were detected in isolated murine cardiomyocytes [82], suggesting $K_v1.2$ may not contribute to I_{ss} in these cells.

The T-tubular fraction of I_{KATP} has, to our knowledge, not yet been determined. It is however likely that at least one of the I_{KATP}-conducting channels $K_{ir}6.1$ and -6.2 is expressed in T-tubules, since I_{KATP}, as well as I_{K1}, decreases along with the loss of T-tubules in cardiomyocytes that have been taken in culture (reviewed in [5]). $K_{ir}6.2$ has been associated with the T-tubular protein ankyrin-B, although these immunohistochemistry data lack a fiducial T-tubular marker [93].

Considering immunohistochemistry data, T-tubular expression has been shown relatively convincingly for $K_v11.1$ by co-staining with myosin-binding protein C [94]. A thorough live-cell imaging study for $K_v2.1$ and $K_v1.4$ in rat cardiomyocytes shows a T-tubular-like pattern, including axial elements, but unfortunately lacks a T-tubular marker [95]. $K_{ir}2.1$, -2.3, -4.2 and TASK-1 show clear co-localization with the membrane marker wheat germ agglutinin in murine ($K_{ir}2.1$), canine ($K_{ir}2.1$ and -2.3) and rat ($K_v4.2$ and TASK-1) ventricular cardiomyocytes [96-99]. For $K_v4.3$ only a striated pattern was shown without T-tubular marker in canine cells [100]. Note that potassium channel composition probably differs between species, since $K_{ir}2.3$ mRNA was not detected in isolated murine cardiomyocytes [82] while $K_{ir}2.3$ protein was found in in canine cells [97]. Interestingly, TASK-1 has been recently defined as an atrial-specific current [101], which seems to contradict these immunohistochemistry and mRNA expression data – although it must be noted that we did not find any recordings of ventricular TASK-1 currents in the literature.

3.4.4 Other ion-handling proteins

Chloride channels are not well researched in T-tubules. Scanning ion conductance microscopy (SICM) experiments revealed that these channels are close to the openings of T-tubules at the lateral membrane [102]. mRNA data show that the voltage-sensitive chloride channels CLCN4, -7, -3, -6 and -1 are expressed in murine ventricular myocytes (in order of expression level) [82], but their roles in cardiac physiology remain to be investigated.

Another ion channel family which roles in cardiac physiology are just emerging is the transient receptor potential (TRP) superfamily of non-selective cation channels. The vanilloid subfamily member TRPV4 is expressed in T-tubules of aged mice and human cardiomyocytes [103]. This is based on immunohistochemistry data in which TRPV4 and the membrane marker caveolin-3 are co-stained. TRPV4 seems to play a role in calcium cycling, but in the aged heart it may contribute to stress-induced cell damage. Of note, TRPV4-encoding mRNA is not found in murine cardiomyocytes [82], which illustrates that even among mouse models, ion channel composition may differ.

3.5 Ion dynamics in T-tubules

The small luminal space of T-tubules can affect the ion diffusion and therefore the driving force of ion channels (discussed in **Section 3.2**). Diffusion rates of ions are slower in T-tubules than in other extracellular spaces, with a markedly higher delay for divalent than monovalent ions [18, 19]. Functionally, an extracellular change in calcium concentration reaches the T-tubules 2.3 seconds later in guinea pig cardiomyocytes, indicating a "fuzzy space" [104]. This diffusion delay is related to the membrane microfolds that are shaped by Bin1 [42]. These microfolds are proposed to protect against arrhythmias, since excitability of the cell would increase when ions can diffuse faster (reviewed in [5]). The finding that T-tubules of animals with higher heart rates are narrower than in low-heart-rate animals [5] might indicate that the relatively high calcium depletion and potassium accumulation rates in the narrow tubules of high-heart-rate animals are of evolutionary benefit.

Theoretically, calcium influx during an action potential may deplete the T-tubular lumen of calcium and reduce the driving force of the calcium channel. This may cause self-attenuation of the calcium current and thus shorten the action potential [45], in a manner similar to what was proposed in the context of intercalated discs for the late sodium current during the plateau phase (see **Section 3.2**) [62]: the sooner the calcium channels close, the sooner the potassium current repolarizes the membrane. A strong depletion of calcium and accumulation of potassium in the T-tubular lumen is however unlikely due to the physiological need for significant electrochemical gradients of calcium and potassium, which will be secured by NCX and

NKA [74]. An important general remark is that we cannot speak of a shorter or longer action potential in T-tubules compared to the rest of the sarcolemma as one might think from the finding that detubulated rat cells show shorter action potentials due to the lost calcium current [26]. The membrane domains of the cell are electrically too tightly coupled [105, 106]. Detubulation may however affect action potential duration of other species differently as rat cardiomyoyctes show a relatively unique calcium handling profile compared to other mammals, which is partly explained by a reduced NCX/SERCA2a ratio [67].

3.6 T-tubular remodeling in disease

Heart failure has been associated with T-tubular remodeling, characterized by T-tubular widening and an increase in tortuosity [107], the loss of the microfold regulator Bin1 [42], collagen deposition in T-tubules [11, 51], dyad uncoupling [108], physical obstruction of T-tubules [47], and sheet-like T-tubular remodeling in end-stage heart failure [36].

The loss of Bin1 observed in human heart failure has been suggested to be arrhythmogenic as Bin1 knockout mice show a loss of microfolds and are more vulnerable to arrhythmias due to changes in ion dynamics as discussed in **Section 3.5** [42]. Sheet-like remodeling is similarly expected to be arrhythmogenic [36]. On the other hand, collagen deposition in T-tubules, which is also seen in human heart failure, and physical obstruction of T-tubules would again slow ion diffusion [10, 11, 51]. Understanding the interplay of these effects will need further investigation.

T-tubular remodeling likely disturbs optimal excitation-contraction coupling as calcium dynamics greatly depend on T-tubular microstructure [109] and on the association and membrane expression of voltage-gated calcium channels and the sodium-calcium exchanger [110]. Indeed, a hallmark of T-tubular dysfunction is the increase in orphaned RyR2 at the Z-lines [108]. This causes a dysregulation of calcium release as diffusion distances for calcium increase, and the calcium transient slows and broadens. In turn, contraction of the cell desynchronizes and slows. Expectedly, detubulated cardiomyocytes show comparable contraction kinetics as failing cells (reviewed in [10]). Interestingly, in end-stage heart failure patients, relieving the mechanical load with a left-ventricular assist device (LVAD) improves cardiac function but only if the T-tubular system is intact, suggesting that calcium handling deficits may be reversible whereas sheet-like T-tubular remodeling is not [36].

It may be valuable to compare depolarization delays in T-tubules from healthy and diseased cells to assess the passive electrical effects of T-tubular remodeling, although other processes associated with T-tubular remodeling may play greater roles in pathophysiology. Since heart failure is also associated with a reduction of Bin1 expression, and Bin1 is important for voltage-gated calcium channel trafficking to the T-tubules

[33], the resulting dysregulation of this trafficking may further impair calcium dynamics. In summary, the T-tubular remodeling associated with heart failure probably affects cardiomyocyte function via different pathways, yet the effects of T-tubular remodeling on T-tubular depolarization remains to be determined.

4. T-tubules in atrial cardiomyocytes

Although T-tubules support a high heart rate in mammalian ventricular cardiomyocytes, heart rates of atrial cells are just as high with a far less dense T-tubular system [20]. Atrial cells in many species can be subdivided in three sub-populations based on their T-tubular network: dense, semi-dense and disorganized, or absent [8]. In pig and rat atria, cardiomyocytes with a well-organized T-tubular network populated the epicardial layer, whereas the endocardial layer mostly contained empty cardiomyocytes [111]. The degree of tubulation furthermore correlated well with synchronicity of calcium release. This may suggest that T-tubules at the epicardial layer are involved in synchronizing the contraction across the atrial wall [111], and that β-adrenergic stimulation has a faster and greater effect on cells close to the epicardium. Interestingly, one recent study [112] reports that human and murine atrial cardiomyocytes contain relatively many axial tubules, which run over the long axis of the cell. The sparse transverse tubules conduct the excitation of the cell from the surface sarcolemma to the axial tubules, while axial tubules contain much more dyads than transverse tubules, thus allowing quick excitation-contraction coupling around these axial tubules [112].

5. Discussion

This work assessed passive and active electrical properties of T-tubules from which we distilled the physiological function of T-tubules. Generally, the roles of T-tubules are twofold: firstly, T-tubules provide a large calcium-handling stage to allow the cardiomyocyte to generate a relatively high force, and secondly, the relatively large membrane surface facilitates the cell to respond faster to signaling molecules than non-tubulated cells. Importantly, T-tubules are not crucial to sustain a high heart rate – atrial cardiomyocytes contract just as fast [20], and non-tubulated cardiomyocytes from certain avian species even faster [113, 114]. Within mammalian ventricular cardiomyocytes however there is a relationship between heart rate and T-tubular density.

The publications discussed in this review strengthen the hypothesis that T-tubules facilitate rapid and efficient excitation-contraction coupling throughout the entire volume of the cell [26]. The length constant of ~ 68 μm [51] and time constant of ~ 200 μs [58] indicate that electrotonic responses allow depolarization of the entire T-tubular membrane within physiological timescales.

When assessing conduction velocity in cardiac tissue, T-tubules most likely slow conduction from a theoretical point of view. Since a tubulated cardiomyocyte has a greater membrane surface, this additional capacitive load may slow down and delay depolarization. Ion channels in T-tubules, especially Na_v channels, will mitigate this delay. Given that the concentration of Na_v channels in the T-tubule is most likely lower than that in the surface sarcolemma, and assuming T-tubular membrane accounts for 50% of the membrane (which is the case at least in mice and rats [30]), T-tubules will slow down conduction velocity by 29-50%, while loss of T-tubules may accelerate conduction.

Next, we evaluated evidence regarding the expression of voltage-gated sodium channels in the T-tubules. Some neuronal isoforms seem to be expressed in low levels; especially $Na_v1.6$ seems to be expressed in the T-tubules of a mouse model [89]. It remains unclear if these low levels could carry enough current to initiate an action potential. The expression of neuronal channels moreover varies greatly between species and even mouse strains. Concerning the cardiac isoform $Na_v1.5$, T-tubular expression remains debatable, despite several reports pointing in that direction. Generally, it is important to keep in mind that sodium channels are not required to depolarize T-tubular membranes. The often-used term “action potential propagation” in T-tubules therefore should be interpreted as “either passive or active”.

In terms of repolarizing currents, the expression of voltage-gated potassium channels differs greatly between species and mouse models. It is probable that the expression levels suffice to repolarize the membrane to balance the high expression level of voltage-gated calcium channels. Considering ion channel expression data in general, the authors would like to stress that critical evaluation of research data is pivotal, especially when functional detubulation experiments and immunohistochemistry data are concerned.

In cardiac disease, T-tubules often remodel [9]. As a result, T-tubules widen, the tortuous membrane microfolds disappear, dyads uncouple, T-tubules close off to the extracellular space, calcium transient weakens, and T-tubules may take on a sheet-like shape while collagen content in the lumen is increased.

FINANCIAL STATEMENT

This work was supported by the Swiss National Science Foundation [grant no. 310030_165741; HA group].

AUTHOR CONTRIBUTIONS

Sarah Vermij: conceptualization, methodology, visualization, writing- original draft preparation, reviewing and editing.

Hugues Abriel: supervision, writing- reviewing and editing.

Jan Kucera: visualization, writing- reviewing and editing.

ACKNOWLEDGMENTS

The authors express their gratitude to Prof Stephan Rohr and Prof Ernst Niggli for helpful discussions on physiology; Dr. Jean-Sébastien Rougier for thorough feedback on the manuscript; and Diana Gamborino Uzcanga and Michaela Gazzetto for assistance with basic physics.

REFERENCES

[1] C. Soeller, M.B. Cannell, Examination of the transverse tubular system in living cardiac rat myocytes by 2-photon microscopy and digital image-processing techniques, Circ. Res., 84 (1999) 266-275.
[2] E. Wagner, M.A. Lauterbach, T. Kohl, V. Westphal, G.S. Williams, J.H. Steinbrecher, J.H. Streich, B. Korff, H.T. Tuan, B. Hagen, S. Luther, G. Hasenfuss, U. Parlitz, M.S. Jafri, S.W. Hell, W.J. Lederer, S.E. Lehnart, Stimulated emission depletion live-cell super-resolution imaging shows proliferative remodeling of T-tubule membrane structures after myocardial infarction, Circ. Res., 111 (2012) 402-414. DOI: 10.1161/circresaha.112.274530.
[3] I.D. Jayasinghe, A.H. Clowsley, M. Munro, Y. Hou, D.J. Crossman, C. Soeller, Revealing T-tubules in striated muscle with new optical super-resolution microscopy techniquess, Eur. J. Trans. Myol., 25 (2015) 4747. DOI: 10.4081/ejtm.2015.4747.
[4] C. Pinali, H. Bennett, J.B. Davenport, A.W. Trafford, A. Kitmitto, Three-dimensional reconstruction of cardiac sarcoplasmic reticulum reveals a continuous network linking transverse-tubules: this organization is perturbed in heart failure, Circ. Res., 113 (2013) 1219-1230. DOI: 10.1161/CIRCRESAHA.113.301348.
[5] T. Hong, R.M. Shaw, Cardiac T-tubule microanatomy and function, Physiol. Rev., 97 (2017) 227-252. DOI: 10.1152/physrev.00037.2015.
[6] N.K. Bhogal, A. Hasan, J. Gorelik, The development of compartmentation of cAMP signaling in cardiomyocytes: the role of T-tubules and caveolae microdomains, J. Cardiovasc. Dev. Dis., 5 (2018). DOI: 10.3390/jcdd5020025.
[7] D.M. Bers, Cardiac excitation-contraction coupling, Nature, 415 (2002) 198-205. DOI: 10.1038/415198a.
[8] M.A. Richards, J.D. Clarke, P. Saravanan, N. Voigt, D. Dobrev, D.A. Eisner, A.W. Trafford, K.M. Dibb, Transverse tubules are a common feature in large mammalian atrial myocytes including human, Am. J. Physiol. Heart Circ. Physiol., 301 (2011) H1996-2005. DOI: 10.1152/ajpheart.00284.2011.
[9] D.J. Crossman, I.D. Jayasinghe, C. Soeller, Transverse tubule remodelling: a cellular pathology driven by both sides of the plasmalemma?, Biophys. Rev., 9 (2017) 919-929. DOI: 10.1007/s12551-017-0273-7.
[10] C. Crocini, C. Ferrantini, R. Coppini, L. Sacconi, Electrical defects of the transverse-axial tubular system in cardiac diseases, J. Physiol., 595 (2017) 3815-3822. DOI: 10.1113/JP273042.
[11] D.J. Crossman, X. Shen, M. Jullig, M. Munro, Y. Hou, M. Middleditch, D. Shrestha, A. Li, S. Lal, C.G. Dos Remedios, D. Baddeley, P.N. Ruygrok, C. Soeller, Increased collagen within the transverse tubules in human heart failure, Cardiovasc. Res., 113 (2017) 879-891. DOI: 10.1093/cvr/cvx055.
[12] A.L. Hodgkin, A.F. Huxley, Propagation of electrical signals along giant nerve fibers, Proc R Soc Soc Lond, Ser B: Biol Sci, 140 (1952) 177-183.
[13] A.L. Hodgkin, A.F. Huxley, A quantitative description of membrane current and its application to conduction and excitation in nerve, J. Physiol., 117 (1952) 500-544.
[14] D. Noble, Cardiac action and pacemaker potentials based on the Hodgkin-Huxley equations, Nature, 188 (1960) 495-497.
[15] D. Noble, The voltage dependence of the cardiac membrane conductance, Biophys. J., 2 (1962) 381-393.
[16] R.W. Joyner, Effects of the discrete pattern of electrical coupling on propagation through an electrical syncytium, Circ. Res., 50 (1982) 192-200.

[17] A.G. Kleber, Y. Rudy, Basic mechanisms of cardiac impulse propagation and associated arrhythmias, Physiol. Rev., 84 (2004) 431-488. DOI: 10.1152/physrev.00025.2003.
[18] W.J. Lederer, E. Niggli, R.W. Hadley, Sodium-calcium exchange in excitable cells: fuzzy space, Science, 248 (1990) 283.
[19] F. Swift, T.A. Stromme, B. Amundsen, O.M. Sejersted, I. Sjaastad, Slow diffusion of K+ in the T tubules of rat cardiomyocytes, J. Appl. Physiol., 101 (2006) 1170-1176. DOI: 10.1152/japplphysiol.00297.2006.
[20] S. Brandenburg, E.C. Arakel, B. Schwappach, S.E. Lehnart, The molecular and functional identities of atrial cardiomyocytes in health and disease, Biochim. Biophys. Acta, 1863 (2016) 1882-1893. DOI: 10.1016/j.bbamcr.2015.11.025.
[21] S.H. Vermij, H. Abriel, T.A. van Veen, Refining the molecular organization of the cardiac intercalated disc, Cardiovasc. Res., 113 (2017) 259-275. DOI: 10.1093/cvr/cvw259.
[22] E. Hichri, H. Abriel, J.P. Kucera, Distribution of cardiac sodium channels in clusters potentiates ephaptic interactions in the intercalated disc, J. Physiol., 596 (2018) 563-589. DOI: 10.1113/JP275351.
[23] J.M. Rhett, R. Veeraraghavan, S. Poelzing, R.G. Gourdie, The perinexus: sign-post on the path to a new model of cardiac conduction?, Trends Cardiovasc. Med., 23 (2013) 222-228. DOI: 10.1016/j.tcm.2012.12.005.
[24] R. Veeraraghavan, J. Lin, G.S. Hoeker, J.P. Keener, R.G. Gourdie, S. Poelzing, Sodium channels in the Cx43 gap junction perinexus may constitute a cardiac ephapse: an experimental and modeling study, Pfluegers Arch./Eur. J. Physiol., 467 (2015) 2093-2105. DOI: 10.1007/s00424-014-1675-z.
[25] D. Shy, L. Gillet, J. Ogrodnik, M. Albesa, A.O. Verkerk, R. Wolswinkel, J.S. Rougier, J. Barc, M.C. Essers, N. Syam, R.F. Marsman, A.M. van Mil, S. Rotman, R. Redon, C.R. Bezzina, C.A. Remme, H. Abriel, PDZ domain-binding motif regulates cardiomyocyte compartment-specific NaV1.5 channel expression and function, Circulation, 130 (2014) 147-160. DOI: 10.1161/circulationaha.113.007852.
[26] F. Brette, L. Salle, C.H. Orchard, Quantification of calcium entry at the T-tubules and surface membrane in rat ventricular myocytes, Biophys. J., 90 (2006) 381-389. DOI: 10.1529/biophysj.105.069013.
[27] M. Ibrahim, J. Gorelik, M.H. Yacoub, C.M. Terracciano, The structure and function of cardiac t-tubules in health and disease, Proc R Soc Soc Lond, Ser B: Biol Sci, 278 (2011) 2714-2723. DOI: 10.1098/rspb.2011.0624.
[28] A. Sandow, Excitation-contraction coupling in skeletal muscle, Pharmacol. Rev., 17 (1965) 265-320.
[29] C.H.T. Kong, E.A. Rog-Zielinska, P. Kohl, C.H. Orchard, M.B. Cannell, Solute movement in the t-tubule system of rabbit and mouse cardiomyocytes, Proc. Natl. Acad. Sci. USA, 115 (2018) E7073-E7080. DOI: 10.1073/pnas.1805979115.
[30] M. Pasek, F. Brette, A. Nelson, C. Pearce, A. Qaiser, G. Christe, C.H. Orchard, Quantification of t-tubule area and protein distribution in rat cardiac ventricular myocytes, Prog. Biophys. Mol. Biol., 96 (2008) 244-257. DOI: 10.1016/j.pbiomolbio.2007.07.016.
[31] T. Hayashi, M.E. Martone, Z. Yu, A. Thor, M. Doi, M.J. Holst, M.H. Ellisman, M. Hoshijima, Three-dimensional electron microscopy reveals new details of membrane systems for Ca2+ signaling in the heart, J. Cell Sci., 122 (2009) 1005-1013. DOI: 10.1242/jcs.028175.
[32] M. Escobar, C. Cardenas, K. Colavita, N.B. Petrenko, C. Franzini-Armstrong, Structural evidence for perinuclear calcium microdomains in cardiac myocytes, J. Mol. Cell Cardiol., 50 (2011) 451-459. DOI: 10.1016/j.yjmcc.2010.11.021.
[33] Y. Fu, T. Hong, BIN1 regulates dynamic t-tubule membrane, Biochim. Biophys. Acta, 1863 (2016) 1839-1847. DOI: 10.1016/j.bbamcr.2015.11.004.
[34] K.R. Levin, E. Page, Quantitative studies on plasmalemmal folds and caveolae of rabbit ventricular myocardial cells, Circ. Res., 46 (1980) 244-255.
[35] E. Page, Quantitative ultrastructural analysis in cardiac membrane physiology, Am. J. Physiol. Cell Physiol., 235 (1978) C147-158. DOI: 10.1152/ajpcell.1978.235.5.C147.
[36] T. Seidel, S. Navankasattusas, A. Ahmad, N.A. Diakos, W.D. Xu, M. Tristani-Firouzi, M.J. Bonios, I. Taleb, D.Y. Li, C.H. Selzman, S.G. Drakos, F.B. Sachse, Sheet-like remodeling of the transverse tubular system in human heart failure impairs excitation-contraction coupling and functional recovery by mechanical unloading, Circulation, 135 (2017) 1632-1645. DOI: 10.1161/circulationaha.116.024470.
[37] C.A. Makarewich, R.N. Correll, H. Gao, H. Zhang, B. Yang, R.M. Berretta, V. Rizzo, J.D. Molkentin, S.R. Houser, A caveolae-targeted L-type Ca(2)+ channel antagonist inhibits hypertrophic signaling without reducing cardiac contractility, Circ. Res., 110 (2012) 669-674. DOI: 10.1161/circresaha.111.264028.
[38] M. Ibrahim, A. Nader, M.H. Yacoub, C. Terracciano, Manipulation of sarcoplasmic reticulum Ca2+ release in heart failure through mechanical intervention, J. Physiol. (Lond.), 593 (2015) 3253-3259. DOI: 10.1113/Jp270446.
[39] R.J. van Oort, A. Garbino, W. Wang, S.S. Dixit, A.P. Landstrom, N. Gaur, A.C. De Almeida, D.G. Skapura, Y. Rudy, A.R. Burns, M.J. Ackerman, X.H. Wehrens, Disrupted junctional membrane complexes and hyperactive

ryanodine receptors after acute junctophilin knockdown in mice, Circulation, 123 (2011) 979-988. DOI: 10.1161/circulationaha.110.006437.
[40] I. Jayasinghe, A.H. Clowsley, R. Lin, T. Lutz, C. Harrison, E. Green, D. Baddeley, L. Di Michele, C. Soeller, True molecular scale visualization of variable clustering properties of ryanodine receptors, Cell Rep., 22 (2018) 557-567. DOI: 10.1016/j.celrep.2017.12.045.
[41] T.T. Hong, J.W. Smyth, D. Gao, K.Y. Chu, J.M. Vogan, T.S. Fong, B.C. Jensen, H.M. Colecraft, R.M. Shaw, BIN1 localizes the L-type calcium channel to cardiac T-tubules, PLoS Biol., 8 (2010) e1000312. DOI: 10.1371/journal.pbio.1000312.
[42] T. Hong, H. Yang, S.S. Zhang, H.C. Cho, M. Kalashnikova, B. Sun, H. Zhang, A. Bhargava, M. Grabe, J. Olgin, J. Gorelik, E. Marban, L.Y. Jan, R.M. Shaw, Cardiac BIN1 folds T-tubule membrane, controlling ion flux and limiting arrhythmia, Nat. Med., 20 (2014) 624-632. DOI: 10.1038/nm.3543.
[43] S. Dhein, T. Seidel, A. Salameh, J. Jozwiak, A. Hagen, M. Kostelka, G. Hindricks, F.W. Mohr, Remodeling of cardiac passive electrical properties and susceptibility to ventricular and atrial arrhythmias, Front. Physiol., 5 (2014) 424. DOI: 10.3389/fphys.2014.00424.
[44] J.H. King, C.L. Huang, J.A. Fraser, Determinants of myocardial conduction velocity: implications for arrhythmogenesis, Front. Physiol., 4 (2013) 154. DOI: 10.3389/fphys.2013.00154.
[45] M. Pasek, J. Simurda, C.H. Orchard, G. Christe, A model of the guinea-pig ventricular cardiac myocyte incorporating a transverse-axial tubular system, Prog. Biophys. Mol. Biol., 96 (2008) 258-280. DOI: 10.1016/j.pbiomolbio.2007.07.022.
[46] C.H.T. Kong, E.A. Rog-Zielinska, C.H. Orchard, P. Kohl, M.B. Cannell, Sub-microscopic analysis of t-tubule geometry in living cardiac ventricular myocytes using a shape-based analysis method, J. Mol. Cell Cardiol., 108 (2017) 1-7. DOI: 10.1016/j.yjmcc.2017.05.003.
[47] M. Scardigli, C. Crocini, C. Ferrantini, T. Gabbrielli, L. Silvestri, R. Coppini, C. Tesi, E.A. Rog-Zielinska, P. Kohl, E. Cerbai, C. Poggesi, F.S. Pavone, L. Sacconi, Quantitative assessment of passive electrical properties of the cardiac T-tubular system by FRAP microscopy, Proc. Natl. Acad. Sci. USA, 114 (2017) 5737-5742. DOI: 10.1073/pnas.1702188114.
[48] S. Weidmann, The electrical constants of Purkinje fibres, J. Physiol., 118 (1952) 348-360.
[49] J.J.B. Jack, D. Noble, R.W. Tsien, Chapter 10 in: Electric current flow in excitable cells, Clarendon Press, Oxford, 1975, pp. 292-296.
[50] S.H. Vermij, H. Abriel, J.P. Kucera, Modelling depolarization delay, sodium currents, and electrical potentials in cardiac transverse tubules, bioRxiv, (2019) 611558. DOI: 10.1101/611558.
[51] K. Uchida, A.N. Lopatin, Diffusional and electrical properties of T-tubules are governed by their constrictions and dilations, Biophys. J., 114 (2018) 437-449. DOI: 10.1016/j.bpj.2017.11.3742.
[52] R.R. Poznanski, A generalized tapering equivalent cable model for dendritic neurons, Bull. Math. Biol., 53 (1991) 457-467.
[53] S.S. Goldstein, W. Rall, Changes of action potential shape and velocity for changing core conductor geometry, Biophys. J., 14 (1974) 731-757. DOI: 10.1016/S0006-3495(74)85947-3.
[54] W. Rall, Theory of physiological properties of dendrites, Ann. N. Y. Acad. Sci., 96 (1962) 1071-1092.
[55] A. Gopinathan, Neuronal space constants in various geometries and physiological conditions, arXiv, (2013).
[56] W. Rall, Electrophysiology of a dendritic neuron model, Biophys. J., 2 (1962) 145-167.
[57] N. Shepherd, H.B. McDonough, Ionic diffusion in transverse tubules of cardiac ventricular myocytes, Am. J. Physiol., 275 (1998) H852-860.
[58] L.F. Cheng, F. Wang, A.N. Lopatin, Metabolic stress in isolated mouse ventricular myocytes leads to remodeling of t tubules, Am. J. Physiol. Heart Circ. Physiol., 301 (2011) H1984-1995. DOI: 10.1152/ajpheart.00304.2011.
[59] M. Pasek, J. Simurda, G. Christe, The functional role of cardiac T-tubules explored in a model of rat ventricular myocytes, Philos. Trans. A Math. Phys. Eng. Sci., 364 (2006) 1187-1206. DOI: 10.1098/rsta.2006.1764.
[60] A. Hatano, J. Okada, T. Washio, T. Hisada, S. Sugiura, An integrated finite element simulation of cardiomyocyte function based on triphasic theory, Front. Physiol., 6 (2015) 287. DOI: 10.3389/fphys.2015.00287.
[61] Y. Mori, G.I. Fishman, C.S. Peskin, Ephaptic conduction in a cardiac strand model with 3D electrodiffusion, Proc Natl Acad Sci U S A, 105 (2008) 6463-6468. DOI: 10.1073/pnas.0801089105.
[62] A. Greer-Short, S.A. George, S. Poelzing, S.H. Weinberg, Revealing the Concealed Nature of Long-QT Type 3 Syndrome, Circ Arrhythm Electrophysiol, 10 (2017) e004400. DOI: 10.1161/CIRCEP.116.004400.
[63] R.M. Shaw, Y. Rudy, Ionic mechanisms of propagation in cardiac tissue. Roles of the sodium and L-type calcium currents during reduced excitability and decreased gap junction coupling, Circ. Res., 81 (1997) 727-741.
[64] R. Plonsey, R.C. Barr, Chapter 9 in: Bioelectricity, a quantitative approach, Springer, New York, 2007, pp. 267-323.

[65] V. Jacquemet, C.S. Henriquez, Loading effect of fibroblast-myocyte coupling on resting potential, impulse propagation, and repolarization: insights from a microstructure model, Am. J. Physiol. Heart Circ. Physiol., 294 (2008) H2040-2052. DOI: 10.1152/ajpheart.01298.2007.
[66] A.F. Huxley, Ion movements during nerve activity, Ann. N. Y. Acad. Sci., 81 (1959) 221-246.
[67] F. Brette, C.H. Orchard, Density and sub-cellular distribution of cardiac and neuronal sodium channel isoforms in rat ventricular myocytes, Biochem. Biophys. Res. Commun., 348 (2006) 1163-1166. DOI: 10.1016/j.bbrc.2006.07.189.
[68] D. Platzer, K. Zorn-Pauly, Letter to the editor: Accurate cell capacitance determination from a single voltage step: a reminder to avoid unnecessary pitfalls, Am. J. Physiol. Heart Circ. Physiol., 311 (2016) H1072-H1073. DOI: 10.1152/ajpheart.00503.2016.
[69] H.C. Gadeberg, C.H.T. Kong, S.M. Bryant, A.F. James, C.H. Orchard, Cholesterol depletion does not alter the capacitance or Ca handling of the surface or t-tubule membranes in mouse ventricular myocytes, Physiol Rep, 5 (2017). DOI: 10.14814/phy2.13500.
[70] C.A. Eichel, A. Beuriot, M.Y. Chevalier, J.S. Rougier, F. Louault, G. Dilanian, J. Amour, A. Coulombe, H. Abriel, S.N. Hatem, E. Balse, Lateral membrane-specific MAGUK CASK down-regulates NaV1.5 channel in cardiac myocytes, Circ. Res., 119 (2016) 544-556. DOI: 10.1161/circresaha.116.309254.
[71] S. Dai, D.D. Hall, J.W. Hell, Supramolecular assemblies and localized regulation of voltage-gated ion channels, Physiol. Rev., 89 (2009) 411-452. DOI: 10.1152/physrev.00029.2007.
[72] M. Kawai, M. Hussain, C.H. Orchard, Excitation-contraction coupling in rat ventricular myocytes after formamide-induced detubulation, Am. J. Physiol., 277 (1999) H603-609. DOI: 10.1152/ajpheart.1999.277.2.H603.
[73] D.R. Scriven, P. Dan, E.D. Moore, Distribution of proteins implicated in excitation-contraction coupling in rat ventricular myocytes, Biophys. J., 79 (2000) 2682-2691. DOI: 10.1016/S0006-3495(00)76506-4.
[74] S. Despa, F. Brette, C.H. Orchard, D.M. Bers, Na/Ca exchange and Na/K-ATPase function are equally concentrated in transverse tubules of rat ventricular myocytes, Biophys J, 85 (2003) 3388-3396. DOI: 10.1016/S0006-3495(03)74758-4.
[75] M. Pasek, J. Simurda, G. Christe, Different densities of Na-Ca exchange current in T-tubular and surface membranes and their impact on cellular activity in a model of rat ventricular cardiomyocyte, Biomed Res. Int., 2017 (2017) 6343821. DOI: 10.1155/2017/6343821.
[76] E. Lin, V.H. Hung, H. Kashihara, P. Dan, G.F. Tibbits, Distribution patterns of the Na+-Ca2+ exchanger and caveolin-3 in developing rabbit cardiomyocytes, Cell Calcium, 45 (2009) 369-383. DOI: 10.1016/j.ceca.2009.01.001.
[77] A. Chase, C.H. Orchard, Ca efflux via the sarcolemmal Ca ATPase occurs only in the t-tubules of rat ventricular myocytes, J. Mol. Cell Cardiol., 50 (2011) 187-193. DOI: 10.1016/j.yjmcc.2010.10.012.
[78] P.J. Mohler, I. Rivolta, C. Napolitano, G. LeMaillet, S. Lambert, S.G. Priori, V. Bennett, Nav1.5 E1053K mutation causing Brugada syndrome blocks binding to ankyrin-G and expression of Nav1.5 on the surface of cardiomyocytes, Proc. Natl. Acad. Sci. USA, 101 (2004) 17533-17538. DOI: 10.1073/pnas.0403711101.
[79] J.N. Dominguez, A. de la Rosa, F. Navarro, D. Franco, A.E. Aranega, Tissue distribution and subcellular localization of the cardiac sodium channel during mouse heart development, Cardiovasc. Res., 78 (2008) 45-52. DOI: 10.1093/cvr/cvm118.
[80] D. Ponce-Balbuena, G. Guerrero-Serna, C.R. Valdivia, R. Caballero, F.J. Diez-Guerra, E.N. Jimenez-Vazquez, R.J. Ramirez, A. Monteiro da Rocha, T.J. Herron, K.F. Campbell, B.C. Willis, F.J. Alvarado, M. Zarzoso, K. Kaur, M. Perez-Hernandez, M. Matamoros, H.H. Valdivia, E. Delpon, J. Jalife, Cardiac Kir2.1 and NaV1.5 channels traffic together to the sarcolemma to control excitability, Circ. Res., 122 (2018) 1501-1516. DOI: 10.1161/circresaha.117.311872.
[81] J.S. Rougier, H. Abriel, Role of "non-cardiac" voltage-gated sodium channels in cardiac cells, J. Mol. Cell Cardiol., 53 (2012) 589-590. DOI: 10.1016/j.yjmcc.2012.08.011.
[82] M. Chevalier, S.H. Vermij, K. Wyler, L. Gillet, I. Keller, H. Abriel, Transcriptomic analyses of murine ventricular cardiomyocytes, Sci. Data, 5 (2018) 180170. DOI: 10.1038/sdata.2018.170.
[83] F. Brette, C.H. Orchard, No apparent requirement for neuronal sodium channels in excitation-contraction coupling in rat ventricular myocytes, Circ. Res., 98 (2006) 667-674. DOI: 10.1161/01.RES.0000209963.02720.70.
[84] S.K. Maier, R.E. Westenbroek, K.A. McCormick, R. Curtis, T. Scheuer, W.A. Catterall, Distinct subcellular localization of different sodium channel alpha and beta subunits in single ventricular myocytes from mouse heart, Circulation, 109 (2004) 1421-1427. DOI: 10.1161/01.CIR.0000121421.61896.24.
[85] S.K. Maier, R.E. Westenbroek, K.A. Schenkman, E.O. Feigl, T. Scheuer, W.A. Catterall, An unexpected role for brain-type sodium channels in coupling of cell surface depolarization to contraction in the heart, Proc. Natl. Acad. Sci. USA, 99 (2002) 4073-4078. DOI: 10.1073/pnas.261705699.

[86] M. Koleske, I. Bonilla, J. Thomas, N. Zaman, S. Baine, B.C. Knollmann, R. Veeraraghavan, S. Gyorke, P.B. Radwanski, Tetrodotoxin-sensitive Navs contribute to early and delayed afterdepolarizations in long QT arrhythmia models, J. Gen. Physiol., 150 (2018) 991-1002. DOI: 10.1085/jgp.201711909.
[87] R.E. Westenbroek, S. Bischoff, Y. Fu, S.K. Maier, W.A. Catterall, T. Scheuer, Localization of sodium channel subtypes in mouse ventricular myocytes using quantitative immunocytochemistry, J. Mol. Cell Cardiol., 64 (2013) 69-78. DOI: 10.1016/j.yjmcc.2013.08.004.
[88] C. Marionneau, C.F. Lichti, P. Lindenbaum, F. Charpentier, J.M. Nerbonne, R.R. Townsend, J. Merot, Mass spectrometry-based identification of native cardiac Nav1.5 channel alpha subunit phosphorylation sites, J. Proteome Res., 11 (2012) 5994-6007. DOI: 10.1021/pr300702c.
[89] S.F. Noujaim, K. Kaur, M. Milstein, J.M. Jones, P. Furspan, D. Jiang, D.S. Auerbach, T. Herron, M.H. Meisler, J. Jalife, A null mutation of the neuronal sodium channel NaV1.6 disrupts action potential propagation and excitation-contraction coupling in the mouse heart, FASEB J., 26 (2012) 63-72. DOI: 10.1096/fj.10-179770.
[90] P.B. Radwanski, H.T. Ho, R. Veeraraghavan, L. Brunello, B. Liu, A.E. Belevych, S.D. Unudurthi, M.A. Makara, S.G. Priori, P. Volpe, A.A. Armoundas, W.H. Dillmann, B.C. Knollmann, P.J. Mohler, T.J. Hund, S. Gyorke, Neuronal Na(+) channels are integral components of pro-arrhythmic Na(+)/Ca(2+) signaling nanodomain that promotes cardiac arrhythmias during beta-adrenergic stimulation, JACC Basic Transl. Sci., 1 (2016) 251-266. DOI: 10.1016/j.jacbts.2016.04.004.
[91] G.K. Yuen, S. Galice, D.M. Bers, Subcellular localization of Na/K-ATPase isoforms in ventricular myocytes, J. Mol. Cell Cardiol., 108 (2017) 158-169. DOI: 10.1016/j.yjmcc.2017.05.013.
[92] K. Komukai, F. Brette, T.T. Yamanushi, C.H. Orchard, K+ current distribution in rat sub-epicardial ventricular myocytes, Pfluegers Arch./Eur. J. Physiol., 444 (2002) 532-538. DOI: 10.1007/s00424-002-0851-8.
[93] J. Li, C.F. Kline, T.J. Hund, M.E. Anderson, P.J. Mohler, Ankyrin-B regulates Kir6.2 membrane expression and function in heart, J. Biol. Chem., 285 (2010) 28723-28730. DOI: 10.1074/jbc.M110.147868.
[94] E.M. Jones, E.C. Roti Roti, J. Wang, S.A. Delfosse, G.A. Robertson, Cardiac IKr channels minimally comprise hERG 1a and 1b subunits, J. Biol. Chem., 279 (2004) 44690-44694. DOI: 10.1074/jbc.M408344200.
[95] K.M. O'Connell, J.D. Whitesell, M.M. Tamkun, Localization and mobility of the delayed-rectifer K+ channel Kv2.1 in adult cardiomyocytes, Am. J. Physiol. Heart Circ. Physiol., 294 (2008) H229-237. DOI: 10.1152/ajpheart.01038.2007.
[96] R.B. Clark, A. Tremblay, P. Melnyk, B.G. Allen, W.R. Giles, C. Fiset, T-tubule localization of the inward-rectifier K(+) channel in mouse ventricular myocytes: a role in K(+) accumulation, J. Physiol., 537 (2001) 979-992.
[97] P. Melnyk, L. Zhang, A. Shrier, S. Nattel, Differential distribution of Kir2.1 and Kir2.3 subunits in canine atrium and ventricle, Am. J. Physiol. Heart Circ. Physiol., 283 (2002) H1123-1133. DOI: 10.1152/ajpheart.00934.2001.
[98] S. Takeuchi, Y. Takagishi, K. Yasui, Y. Murata, J. Toyama, I. Kodama, Voltage-gated K(+) channel, Kv4.2, localizes predominantly to the transverse-axial tubular system of the rat myocyte, J. Mol. Cell Cardiol., 32 (2000) 1361-1369. DOI: 10.1006/jmcc.2000.1172.
[99] S.A. Jones, M.J. Morton, M. Hunter, M.R. Boyett, Expression of TASK-1, a pH-sensitive twin-pore domain K(+) channel, in rat myocytes, Am. J. Physiol. Heart Circ. Physiol., 283 (2002) H181-185. DOI: 10.1152/ajpheart.00963.2001.
[100] I. Deschenes, D. DiSilvestre, G.J. Juang, R.C. Wu, W.F. An, G.F. Tomaselli, Regulation of Kv4.3 current by KChIP2 splice variants: a component of native cardiac I(to)?, Circulation, 106 (2002) 423-429.
[101] C. Schmidt, F. Wiedmann, A.R. Gaubatz, A. Ratte, H.A. Katus, D. Thomas, New targets for old drugs: cardiac glycosides inhibit atrial-specific K2P3.1 (TASK-1) channels, J. Pharmacol. Exp. Ther., 365 (2018) 614-623. DOI: 10.1124/jpet.118.247692.
[102] Y. Gu, J. Gorelik, H.A. Spohr, A. Shevchuk, M.J. Lab, S.E. Harding, I. Vodyanoy, D. Klenerman, Y.E. Korchev, High-resolution scanning patch-clamp: new insights into cell function, FASEB J., 16 (2002) 748-750. DOI: 10.1096/fj.01-1024fje.
[103] J.L. Jones, D. Peana, A.B. Veteto, M.D. Lambert, Z. Nourian, N.G. Karasseva, M.A. Hill, B.R. Lindman, C.P. Baines, M. Krenz, T.L. Domeier, TRPV4 increases cardiomyocyte calcium cycling and contractility yet contributes to damage in the aged heart following hypoosmotic stress, Cardiovasc. Res., (2018). DOI: 10.1093/cvr/cvy156.
[104] L.A. Blatter, E. Niggli, Confocal near-membrane detection of calcium in cardiac myocytes, Cell Calcium, 23 (1998) 269-279.
[105] G. Bu, H. Adams, E.J. Berbari, M. Rubart, Uniform action potential repolarization within the sarcolemma of in situ ventricular cardiomyocytes, Biophys. J., 96 (2009) 2532-2546. DOI: 10.1016/j.bpj.2008.12.3896.
[106] L. Sacconi, C. Ferrantini, J. Lotti, R. Coppini, P. Yan, L.M. Loew, C. Tesi, E. Cerbai, C. Poggesi, F.S. Pavone, Action potential propagation in transverse-axial tubular system is impaired in heart failure, Proc. Natl. Acad. Sci. USA, 109 (2012) 5815-5819. DOI: 10.1073/pnas.1120188109.

[107] D.J. Crossman, A.A. Young, P.N. Ruygrok, G.P. Nason, D. Baddelely, C. Soeller, M.B. Cannell, T-tubule disease: Relationship between t-tubule organization and regional contractile performance in human dilated cardiomyopathy, J. Mol. Cell Cardiol., 84 (2015) 170-178. DOI: 10.1016/j.yjmcc.2015.04.022.
[108] L.S. Song, E.A. Sobie, S. McCulle, W.J. Lederer, C.W. Balke, H. Cheng, Orphaned ryanodine receptors in the failing heart, Proc. Natl. Acad. Sci. USA, 103 (2006) 4305-4310. DOI: 10.1073/pnas.0509324103.
[109] P.M. Kekenes-Huskey, Y. Cheng, J.E. Hake, F.B. Sachse, J.H. Bridge, M.J. Holst, J.A. McCammon, A.D. McCulloch, A.P. Michailova, Modeling effects of L-type ca(2+) current and na(+)-ca(2+) exchanger on ca(2+) trigger flux in rabbit myocytes with realistic T-tubule geometries, Front. Physiol., 3 (2012) 351. DOI: 10.3389/fphys.2012.00351.
[110] P. Neco, B. Rose, N. Huynh, R. Zhang, J.H. Bridge, K.D. Philipson, J.I. Goldhaber, Sodium-calcium exchange is essential for effective triggering of calcium release in mouse heart, Biophys. J., 99 (2010) 755-764. DOI: 10.1016/j.bpj.2010.04.071.
[111] M. Frisk, J.T. Koivumaki, P.A. Norseng, M.M. Maleckar, O.M. Sejersted, W.E. Louch, Variable t-tubule organization and Ca2+ homeostasis across the atria, Am. J. Physiol. Heart Circ. Physiol., 307 (2014) H609-620. DOI: 10.1152/ajpheart.00295.2014.
[112] S. Brandenburg, J. Pawlowitz, F.E. Fakuade, D. Kownatzki-Danger, T. Kohl, G.Y. Mitronova, M. Scardigli, J. Neef, C. Schmidt, F. Wiedmann, F.S. Pavone, L. Sacconi, I. Kutschka, S. Sossalla, T. Moser, N. Voigt, S.E. Lehnart, Axial tubule junctions activate atrial Ca(2+) release across species, Front. Physiol., 9 (2018) 1227. DOI: 10.3389/fphys.2018.01227.
[113] S. Perni, V.R. Iyer, C. Franzini-Armstrong, Ultrastructure of cardiac muscle in reptiles and birds: optimizing and/or reducing the probability of transmission between calcium release units, J. Muscle Res. Cell Motil., 33 (2012) 145-152. DOI: 10.1007/s10974-012-9297-6.
[114] E.P. Odum, Variations in the heart rate of birds: a study in physiological ecology, Ecol. Monogr., 11 (1941) 299-326.